Fabry–Perot interferometer embedded in a glass chip fabricated by femtosecond laser

Cheng-Hsiang Lin,[1,2] Lan Jiang,[3] Hai Xiao,[4] Yen-Hsin Chai,[5] Shean-Jen Chen,[1] and Hai-Lung Tsai[2,*]

[1]*Department of Engineering Science, National Cheng Kung University, Tainan 70101, Taiwan*
[2]*Department of Mechanical and Aerospace Engineering, Missouri University of Science and Technology, Rolla, Missouri 65409, USA*
[3]*Department of Mechanical and Automation Engineering, 3rd School, Beijing Institute of Technology, Beijing 100081, China*
[4]*Department of Electrical and Computer Engineering, Missouri University of Science and Technology, Rolla, Missouri 65409, USA*
[5]*Department of Electrical Engineering, Technology and Science Institute of Northern Taiwan, Taipei 112, Taiwan*
**Corresponding author: tsai@mst.edu*

Received May 11, 2009; revised July 1, 2009; accepted July 9, 2009;
posted July 15, 2009 (Doc. ID 111175); published August 4, 2009

We report a simple Fabry–Perot interferometer (FPI) embedded in a glass chip, which is capable of precisely measuring the refractive indices of liquid samples. The microdevice is the integration of a single-mode optical fiber and a microchannel in the photosensitive glass fabricated by femtosecond laser followed by thermal treatment, wet etching, and annealing. The function of the FPI is demonstrated by measuring the refractive indices of water and methanol. The interference visibility is more than 4.0 dB, which is sufficient for most sensing applications. This refractive index sensor with rigid structure could be further integrated to become a more complex 3D lab-on-a-chip for reliable biomedical applications. © 2009 Optical Society of America

OCIS codes: 050.2230, 060.2370, 120.3180, 140.7090.

Fiber-based Fabry–Perot interferometers (FPIs) have been used as optical sensors [1–3] with the advantages of a wide application range, a linear response, and a simple structure. Recently, a technique using a femtosecond laser to precisely fabricate micro-optical devices on glass materials has attracted much interest [4]. Based on the technique, an FPI machined by femtosecond laser directly on an optical fiber was demonstrated by Rao *et al.* [5] and our group [6,7]. However, the brittle fiber glass and the possible bending damage restrict the reliability and the applications of the fiber-based FPI.

The development of "lab-on-a-chip" in analytical chemistry and biomedical applications has resulted in low reagent consumption, fast analysis, compactness of the system, etc. [8]. The Foturan glass, which carries features of optical transparence and resistance to corrosion machined by a femtosecond laser, realizes the top–down one-step fabrication of 3D structures without additional assembly. It greatly simplifies the chip fabrication and is easier to achieve a complex design. In this work, we employ the femtosecond laser direct writing technique to fabricate an FPI that includes an optical fiber and a microchannel embedded in the Foturan glass. As compared with the fiber-based FPI [5–7], the rigid structure of the lab-on-a-chip overcomes the brittle nature of fiber glass, improves the reliability, and maintains the same functionality and compactness.

The schematic of the FPI device is illustrated in Fig. 1. As there is a long buffer region behind the microchannel, multiple reflections can be reduced or eliminated. The FPI can thus be modeled by the following two-beam optical interference equation [9]:

$$I(\lambda) = I_1(\lambda) + I_2(\lambda) + 2\sqrt{I_1(\lambda)I_2(\lambda)}\cos\left(\frac{4\pi nL}{\lambda} + \phi_0\right), \quad (1)$$

where $I(\lambda)$ is the intensity of the interference signal at a specific wavelength, λ is the optical wavelength in vacuum, $I_1(\lambda)$ and $I_2(\lambda)$ are the reflection intensities at each end face of the cavity, ϕ_0 is the initial phase of the interference, L is the cavity length, and n is the refractive index of the medium in the cavity. According to Eq. (1), the two adjacent interference minima have a phase difference of 2π. Therefore, the optical length of the cavity can be calculated by

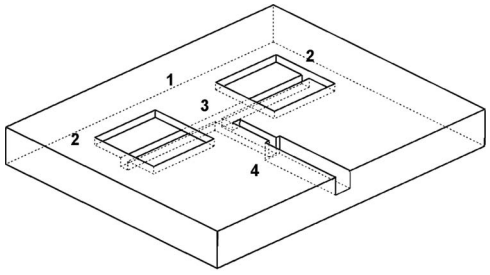

(a)

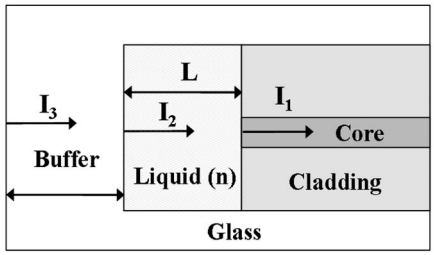

(b)

Fig. 1. Schematic of the FFPI embedded in a glass chip. (a) Chip overview: 1, buffer region; 2, sample inlet and outlet ports; 3, microfluidic channel; 4, fiber holder. (b) Schematic of the FPI (dimensions are not to scale).

0146-9592/09/162408-3/$15.00

$$nL = \frac{1}{2}\left(\frac{\lambda_{v1}\lambda_{v2}}{\lambda_{v2} - \lambda_{v1}}\right), \quad (2)$$

where λ_{v1} and λ_{v2} are the wavelengths of two adjacent valleys in the interference spectrum. Equation (2) can be used to calculate either the absolute refractive index (n) or the absolute length of the cavity (L) if one of them is known.

The direct writing was carried out with a femtosecond laser micromachining system, which consists of a femtosecond laser (Legend-F, Coherent) and a five-axis motion stage (Aerotech) [6]. The pulse energy was adjusted by a combination of a half-wave plate and a polarizer. The attenuated laser beam was directed into a microscope objective lens (Olympus) and focused on the sample, which was translated by the motion stage.

As shown in Fig. 1, the FPI microchip includes three parts: sample inlet and outlet ports, a microchannel, and a fiber holder. The sample inlet and the outlet ports are each 1 mm $\times$ 1 mm square and 0.2 mm deep. The square microchannel, 120 μm $\times$ 120 μm, is 1 mm long, and the center line of the channel is at the distance of 160 μm below the surface. The fiber holder has a 300-μm-long fiber clamp followed by a 5-mm-long open groove. These microcomponents were fabricated in a Foturan glass, which is doped with a trace amount of silver and cerium [10]. By exposure to tightly focused femtosecond light, some silver ions form silver atoms by capturing electrons released from the cerium (Ce^{3+}) ions. In a subsequent heat treatment, the silver atoms agglomerate to form clusters, and then the crystalline phase of lithium metasilicate grows around the silver clusters, which can be preferentially etched away in a dilute solution of hydrofluoric acid, leaving behind the microstructures in the glass. After the modification process, the subsequent thermal treatment, wet etching, and annealing were conducted [10]. The average surface roughness of the fabricated microstructures can be less than 1 nm after the annealing process [11].

A single-mode fiber (SMF 28, Corning) with a cleaved end surface was inserted and glued onto the fiber holder using epoxy. During the measurement, a tunable laser source (HP 8168E) was connected to one end of the 3 dB coupler. The output port of the coupler was connected to the fiber, which has been aligned and glued to the microchip. Controlled by a computer, the tunable laser continuously scanned through the wavelength from 1480 to 1520 nm at a 0.5 nm increment. The reflected interference signal was recorded by an optical power meter (Agilent, 8163A).

Figure 2 shows the optical image of the microchip in the Foturan glass before inserting the optical fiber. Note that the light reflected from the boundary of the glass chip [I_3 in Fig. 1(b)] may affect the spectra because of the high transmittance of the smooth surfaces of the cavity. To eliminate possible multiple reflections of I_3, a 30-mm-long buffer region was used, and the contribution of multiple reflections was found to be negligible. In Eq. (2), the refractive index measurement is based on the known cavity length. To determine the cavity length at different temperatures, the microchip was placed on a temperature controlled hot plate, and the interference spectra were recorded in air at room temperature (23°C) and from 30 to 100°C with a 10°C increment. The background loss of the device is about 23 dB, and the visibility is about 1.5 dB. The relatively low visibility of the interference spectrum is due to the long cavity length and to the nonperfect perpendicular surface of the inserted fiber during the assembling process. Figure 3 shows the measured cavity length as a function of temperature using $n = 1.0003$ for air at the wavelength of 1550 nm [12]. The cavity length increases from 120.220 to 120.799 μm as the temperature increases from 23°C to 100°C. The slope of the cavity length as a function of temperature is found to be 7.7 nm/°C. As the thermal expansion coefficient of the Foturan glass is 8.6×10^{-6}/°C at 23°C, the slope of the thermal expansion is 1.032 nm/°C, which is much smaller than the measured slope. The discrepancy might be caused by the material mismatch between the Foturan glass and the optical fiber. The thermal expansion coefficient of optical fiber (fused silica) is only 5.5×10^{-7}/°C. When the temperature increases from 23°C to 100°C, the difference of thermal expansion between the Foturan glass and the fiber for the length of 5 mm can be as high as 3 μm. This could cause the cleaved fiber end to slightly

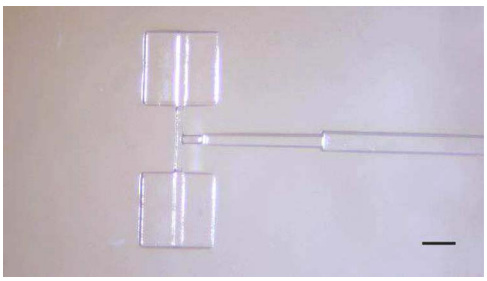

Fig. 2. (Color online) Optical image of the microchip with a 500 μm scale bar.

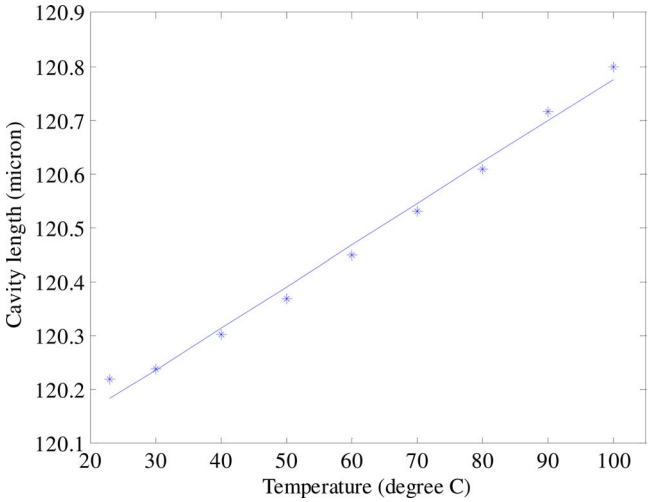

Fig. 3. (Color online) Cavity lengths at different temperatures from 23°C to 100°C.

shrink back into the channel surface as the temperature increases. However, once the temperature cooled down to 23°C, the spectrum returned to the original location and the experiment was well repeatable.

Figure 4 shows the interference spectra of the FPI in air, water, and methanol at room temperature. In Eq. (1), when the intensities of I_1 and I_2 are closer to each other, the visibility of the interference spectra increases. From the Fresnel equation [13], in Fig. 1(b), the intensities of I_1 and I_2 are closer to each other when the refractive index of the medium inside the cavity is closer to the refractive index of the glass. Hence, as shown in Fig. 4 the visibilities of the spectra for both water and methanol were improved to more than 4 dB, which is sufficient for most sensing applications. The spectral distance between the two adjacent valleys also decreases for liquids, indicating that the refractive index of the medium in the cavity is greater than air. Based on the interference spectrum and the known cavity length, the refractive indices of water and methanol were calculated to be 1.3315 and 1.3211, respectively, which are close to the commonly accepted values of 1.32524 [14] and 1.31446 [15]. The discrepancy is mainly caused in the identification of the valleys of the interference spectra. Theoretically, the spectra are cosine waves, but the measured spectra may be distorted and not perfect cosine waves. Because both the cavity length and the refractive indices are determined from the interference spectra, the error would be introduced twice in the calculation.

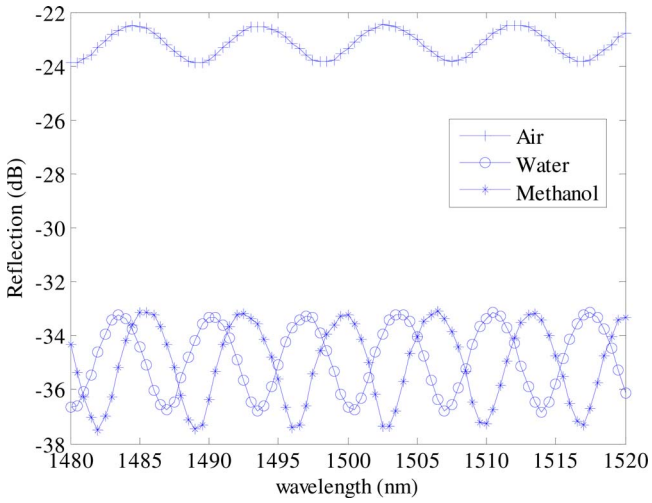

Fig. 4. (Color online) Interference spectra of air, water, and methanol at 23°C.

In conclusion, an on-chip fiber-assisted FPI with a microchannel fabricated in the Foturan glass for highly sensitive refractive index measurements was demonstrated. The cavity lengths at temperatures from 23°C to 100°C were determined. Based on the known cavity length, the device was evaluated by measuring the refractive indices of water and methanol. The visibility of the interference spectrum is improved to more than 4 dB, which is sufficient for most sensing applications. The new lab-on-a-chip design overcomes the brittle nature of the optical fiber and enhances the rigidity and the reliability for practical applications.

References

1. Y. J. Rao, Opt. Fiber Technol. **12**, 227 (2006).
2. J. L. Elster, M. E. Jones, M. K. Evans, S. M. Lenahan, and C. A. Boyce, Proc. SPIE **3911**, 105 (2000).
3. Y. Zhang, H. Shibru, K. L. Cooper, and A. Wang, Opt. Lett. **30**, 1021 (2005).
4. C. B. Schaffer, E. Mazur, and J. A. Squier, Proc. SPIE **4633**, 112 (2002).
5. Y. J. Rao, M. Deng, D. W. Duan, X. C. Yang, T. Zhu, and G. H. Cheng, Opt. Express **15**, 14123 (2007).
6. T. Wei, Y. Han, H. L. Tsai, and H. Xiao, Opt. Lett. **33**, 536 (2008).
7. T. Wei, Y. Han, H. L. Tsai, and H. Xiao, Opt. Express **16**, 5764 (2008).
8. S. K. Hsiung, C. H. Lin, and G. B. Lee, Electrophoresis **26**, 1122 (2005).
9. B. Qi, G. R. Pickrell, J. Xu, P. Zhang, Y. Duan, W. Peng, Z. Huang, W. Huo, H. Xiao, R. G. May, and A. Wang, Opt. Eng. (Bellingham) **42**, 3165 (2003).
10. T. Hongo, K. Sugioka, H. Niino, Y. Cheng, M. Masuda, I. Miyamoto, H. Takai, and K. Midorikawa, J. Appl. Phys. **97**, 063517 (2005).
11. Y. Cheng, K. Sugioka, and K. Midorikawa, Opt. Lett. **28**, 1144 (2003).
12. G. Z. Xiao, A. Adnet, Z. Y. Zhang, F. G. Sun, and C. P. Grover, Sens. Actuators A **118**, 177 (2005).
13. F. L. Pedrotti, L. Pedrotti, L. M. Pedrotti, and L. S. Pedrotti, *Introduction to Optics* (Benjamin Cummings, 2006).
14. H. El-Kashef, Physica B **279**, 295 (2000).
15. P. Schiebener, J. Straub, J. M. H. Levelt Sengers, and J. S. Gallagher, J. Phys. Chem. Ref. Data **19**, 677 (1990).